Journal of Thermal Analysis and Calorimetry, Vol. 73 (2003) 347–359

SALICYLIDENE-2-AMINOBENZIMIDAZOLE SCHIFF BASE COMPLEXES OF Fe(III), Co(II), Ni(II), Cu(II), Zn(II) AND Cd(II)

G. G. Mohamed[1*] *and Z. H. Abd El-Wahab*[2]

[1]Chemistry Department, Faculty of Science, Cairo University, Giza, Egypt
[2]Chemistry Department, Faculty of Science, Azhar University, Nasr City, Egypt

(Received March 25, 2003; in revised form May 18, 2003)

Abstract

New metal complexes of Fe(III), Co(II), Ni(II), Cu(II), Zn(II) and Cd(II) with salicylidene-2-aminobenzimidazole (SABI) are synthesized and their physicochemical properties are investigated using elemental and thermal analyses, IR, conductometric, solid reflectance and magnetic susceptibility measurements. The base reacts with these metal ions to give 1:1 (Metal:SABI) complexes; in cases of Fe(III), Co(II), Cu(II), Zn(II) and Cd(II) ions; and 1:2 (Metal:SABI) complexes; in case of Ni(II) ion. The conductance data reveal that Fe(III) complex is 2:1 electrolyte, Co(II) is 1:2 electrolyte, Cu(II), Zn(II) and Cd(II) complexes are 1:1 electrolytes while Ni(II) is non-electrolyte. IR spectra showed that the ligand is coordinated to the metal ions in a terdentate mannar with O, N, N donor sites of the phenolic –OH, azomethine –N and benzimidazole –N3. Magnetic and solid reflectance spectra are used to infer the coordinating capacity of the ligand and the geometrical structure of these complexes. The thermal decomposition of the complexes is studied and indicates that not only the coordinated and/or crystallization water is lost but also that the decomposition of the ligand from the complexes is necessary to interpret the successive mass loss. Different thermodynamic activation parameters are also reported, using Coats-Redfern method.

Keywords: electronic and magnetic spectra, IR analysis, salicylidene-2-aminobenzimidazole, thermal anlysis, transition metal complexes

Introduction

The field of Schiff base complexes was fast developing on account of the wide variety of possible structures for the ligands depending upon the aldehydes and amines. Many attempts were done to prepare symmetric polydentate ligands in order to achieve rare coordination number with divalent metal ions whose importance was mainly due to their ability to form metal chelates. Even though many Schiff bases using salicyaldehyde and substituted salicyaldehydes and amines had been studied [1–4], as ligands, no work had been done with salicyaldehyde and 2-amino-benzimidazole as the basic nucleus of Schiff

---

[*] Author for correspondence: E-mail: ggenidy@hotmail.com

1388–6150/2003/ $ 20.00

Akadémiai Kiadó, Budapest
Kluwer Academic Publishers, Dordrecht

bases. Schiff base metal complexes had been a widely studied subject due to their industrial and biological applications [5]. Because of new interesting applications found in the field of pesticides and medicine, the metal complexes with tridentate O, N, N or O, N, S types of alternative structures had attracted the attention of chemists [6, 7]. Cu-Schiff base complexes derived from cyclocondensation of benzaldehyde and salicylaldehyde with, α,ω-diamines were afforded to prepare heterobinuclear complexes with molybdenum nitrosyl compounds [8]. The crystal structure of two mononuclear cadmium and a dinuclear, μ-hydroxy-bridged zinc macrocyclic Schiff base complexes were reported [9]. The oxidation chemistry of three Ni(II) complexes with Schiff base ligands derived from salicylaldehyde and diamines with different steric demands were studied by cyclic voltammetry and chronoamperometry [10]. Multidentate imidazole derivatives were known for their chelating abilities for transition metal ions. Detailed studies on the nature of bonding and molecular structures of the metal complexes of benzimidazole derivatives were available [11]. Also, multidentate benzimidazole ligands were incorporated in cross linked polymeric matrices and their ligating behaviour towards different metal ions to develop new types of chelating ion-exchange resin systems were studied [12]. The development of such polymeric ligands could be useful to study the reaction mechanisms in the biological systems involving imidazole and benzimidazole derivatives [13].

The main target of the present study is to synthesize new Schiff base-metal complexes and determine the coordination capacity of a highly coloured benzimidazole Schiff base derivative of salicylidene-2-aminobenzimidazole (SABI) that incorporates several binding sites. The coordination behaviour of SABI towards transition metal salts is investigated via the IR, magnetic moment and solid reflectance spectra measurements. The thermal decomposition of the complexes is also used to infer the structure and the different thermodynamic activation parameters are calculated.

Experimental

Synthesis of the salicylidene-2-aminobenzimidazole (SABI)

This Schiff base was prepared by mixing equimolar amounts of 2-aminobenzimidazole and the aromatic aldehyde in ethanol. The mixture was refluxed for about 5 hours. The yellow crystals of the Schiff base that separated on cooling were recrystallized from ethanol. The yellow Schiff base product obtained (m.p. 140±2°C) was produced in 85% yield and subjected to elemental analyses [Calcd. for $C_{14}H_{11}N_3O$: C, 70.89; H, 4.64; N, 17.72%. Anal. Found: C, 70.30; H, 4.40; N, 17.35%].

Synthesis of the complexes

The metal-salicylidene-2-aminobenzimidazole complexes were prepared by adding 25 mL salicylidene ethanol-water (1:1) solutions of the appropriate metal chloride (Fe(III), Ni(II), Co(II) and Cd(II)) or acetate (Cu(II) and Zn(II)) (0.01 mole) to 30 mL 0.01 M solution of the Schiff base in the same solvent. The resulting mixture was stirred under re-

Table 1 Analytical and physical data of salicylidene-2-aminobenzimidazole and its complexes

Compounds	Colour/ (yield/%)	*M.p.*/°C	Found (calcd.)/%			μ_{eff}/ B.M.	Λ_m/ Ω^{-1} cm^2 mol^{-1}
			C	H	N		
$[H_2L]$	yellow	140±2	70.30	4.40	17.35	–	–
$(C_{14}H_{11}N_3O)$	(85)		(70.89)	(4.64)	(17.72)		
$[Fe(HL)(H_2O)_3](Cl)_2{\cdot}3H_2O$	dark brown	>300	35.29	4.73	8.47	4.60	270
$C_{14}H_{22}N_3O_7Cl_2Fe$	(70)		(35.67)	(4.67)	(8.92)		
$[Co(H_2L)(H_2O)_3](Cl)_2{\cdot}3H_2O$	green	>300	35.62	4.73	8.65	5.40	210
$C_{14}H_{23}N_3O_9Cl_2Co$	(72)		(34.44)	(4.85)	(8.86)		
$[Ni(HL)_2]{\cdot}H_2O$	yellow	>300	61.72	3.95	14.93	3.85	10.2
$C_{28}H_{22}N_6O_3Ni$	(75)		(61.20)	(3.64)	(15.30)		
$[Cu(HL)(H_2O)](OAc)$	yellow	>300	50.85	4.60	10.86	1.92	120
$C_{16}H_{15}N_3O_4Cu$	(82)		(50.99)	(4.25)	(11.16)		
$[Zn(HL)(H_2O)](OAc)$	yellow	>300	50.55	4.07	10.90	Diam.	125
$C_{16}H_{15}N_3O_4Zn$	(76)		(50.79)	(4.23)	(11.11)		
$[Cd(HL)(H_2O)]Cl$	yellow	>300	41.61	3.22	10.13	Diam.	90
$C_{14}H_{12}N_3O_2ClCd$	(82)		(41.84)	(2.99)	(10.46)		

flux for two hours, after which the complexes were precipitated on cooling. They were removed by filtration, washed with 1:1 ethanol:water mixture and with Et_2O.

The analytical data for C, H and N were repeated twice and collected in Table 1. IR spectra were recorded on a Perkin-Elmer FT-IR type 1650 spectrophotometer. The solid reflectance spectra were measured on a Shimadzu 3101 PC spectrophotometer. The conductance measurements were carried out using a Sybron-Barnstead conductometer. The molar magnetic susceptibilities were measured on powdered samples using the Faraday method. The diamagnetic corrections were made by Pascal`s constant. The thermogravimetric analysis (TG) was carried out in dynamic nitrogen atmosphere (20 mL min^{-1}) with a heating rate of 10°C min^{-1} using a Shimadzu TGA-50H thermal analyzer.

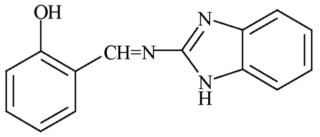

Scheme 1 Structure of salicylidene-2-aminobenzimidazole (H_2L)

Results and discussion

SABI metal complexes

The data obtained in Table 1 show that SABI forms a 1:1 (M:SABI) complexes with Fe(III), Co(II), Cu(II), Zn(II) and Cd(II) ions and 1:2 (M:SABI) complex with Ni(II) ion. The prepared complexes are found to have the general formulae $[M(HL)_z (H_2O)_x]$ (A).yH_2O (M = Fe(III), Ni(II), Cu(II), Zn(II) and Cd(II), A = Cl or OAc, Z = 1 or 2, x = 0–3 and y = 0–3) or $[M(H_2L) (H_2O)_3]Cl_2{\cdot}3H_2O$ (M = Co(II)). The phenolic OH group loses its proton (except for Co(II) complex, where it remains protonated) when coordinated to the metal ions, to serve in reducing the charge on the complex ion. The charge on the complex is neutralized by the presence of chloride or acetate ions in the outersphere of the complex. Thus SABI is expected to fill three coordination positions and contribute a charge of –1. The non involvement of the chloride or acetate ions in the coordination to the metal ions is also confirmed by the conductance measurements.

IR spectra and mode of bonding

The IR spectrum of the ligand shows a broad band at 3450 cm^{-1}, which can be attributed to the phenolic OH group. This band is absent in all the complexes; except Co(II) complex, where the band still in the same position but its intensity is decreased; indicating coordination through the phenolic OH group [14]. Phenolic C-O stretch band is observed at 1306 cm^{-1} in the free ligand. In all complexes, this band appears at higher wavenumber in 1337–1323 cm^{-1} region, confirming the involvement of the phenolic group in complex formation [14]. However, the band due to the azomethine (C=N) group in the free ligand is observed at 1610 cm^{-1} [5, 15]. This band is shifted to lower frequency values upon complexation suggesting coordination via the azomethine group in all of the prepared complexes (M←N). In addition, the ligand exhibits a band at 1378 cm^{-1} due to ν_{cyclic}(C=N) of the imidazole nitrogen (N3). This band is shifted in all the complexes, indicating the involvement of the imidazole (N3) atom in complex formation.

In the far IR spectra of all the complexes, the non-ligand bands observed at 576–518 cm^{-1} region can be assigned to M–N stretch [16]. Conclusive evidence regarding the bonding of oxygen to the metal ions is provided by the occurrence of bands at 438–420 cm^{-1} (M–O) [14].

Therefore, the IR spectra indicate that SABI behaves as monobasic acid and the coordinating sites being Ar–O, –C=N– and –N3 atom of the imidazole ring.

Molar conductivity measurements

By using the relation $\Lambda_m = k/c$, the molar conductivity of the complexes (Λ_m) Ohm^{-1} cm^2 mol^{-1} is calculated usnig 10^{-3} M solutions in DMF. As seen from Table 1, the Schiff base under study forms 1:1 (metal/ligand) complexes with the di- and trivalent metal ions except Ni(II) ion, which forms I:2 complex. The solubility of the complexes in DMF permitted calculation of the molar conductivity (Λ_m) of 10^{-3} M solutions at 25°C [17] and, by comparison, the electrolytic nature for each complex. The molar conductivity for Fe(III) complex is 270 Ohm^{-1} cm^2 mol^{-1} indicating a 2:1 electrolyte and evidences under these circumstances the non-involvement of the chloride in coordination to Fe(III) ion. On the other hand, the low conductivity value of the Ni(II) complex proves its weak molecular nature. The conductance data in Table 1 also indicate that the Co(II) complex is 1:2 electrolyte while Cu(II), Zn(II) and Cd(II) complexes are 1:1 electrolytes.

Magnetic susceptibility and electronic spectra measurements

The solid reflectance spectrum of the copper complex gives a band at 17667 cm^{-1}, which is consistent with tetrahedral or square planar environment [18]. The magnetic susceptibility measurement of 1.92 B.M. is an indicative of the appearance of the copper complex in a square planar geometry. The solid reflectance spectrum of the nickel complex is consistent with the formation of an octahedral geometry with the appearance of three bands at 20800, 18577 and 7980 cm^{-1} corresponding to the transitions $^3A_{2g}\rightarrow{}^3T_{1g}(P)$,$^3A_{2g}\rightarrow{}^3T_{1g}$ (F) and $^3A_{2g}\rightarrow{}^3T_{2g}$. For the cobalt complex, the reflectance spectrum shows two bands of medium intensity at 20850 and 12070 cm^{-1} which are assigned respectively to the transitions $^4T_{1g}$ (F)→ $^4T_{1g}$ (P) and $^4T_{1g}$ (F)→ $^4T_{2g}$ (F) of an octahedral cobalt complex [19]. Such data, gathered with their magnetic moments (3.85 and 5.40 B.M for Ni(II) and Co(II) complexes, respectively), support hexacoordinate configuration [20]. The magnetic moment of Fe(III) complex has been found to be 4.60 B.M, which was within the range of values corresponding to high spin octahedral complexes of Fe(III) complexes. Zinc and cadmium complexes are diamagnetic and are likely to be of tetrahedral structures.

Thermogravimetric studies (TG)

The TG for the complexes was carried out within a temperature range from room temperature up to 1000°C. Coordinated water molecules are directly bonded to the metal ion and are usually eliminated at higher temperatures than those of hydration [21]. The determined temperature ranges, percent mass losses and thermal effects accompanying the changes in the solid complexes on heating are given in Table 2, which revealed the following findings:

The TG curves of the Fe(III) and Co(II) complexes show a three decomposition steps within the temperature ranges of 50–970 and 25–780°C for Fe(III) and Co(II) complexes, respectively. The first estimated mass losses of 11.75 % (theoretical 11.46 %) and 19.65 % (theoretical 19.09 %) within the temperature range of 50–170 and 25–260°C may be attributed to the loss of three water molecules of hydration for the Fe(III) and Co(II) complexes, respectively. The activation energy for these dehydration steps is equal to 45.76 and 40.24 kJ mol^{-1} for Fe(III) and Co(II) complexes, respectively. The loss of coordinated water and ligand molecules take place within the temperature range of 175–970 and 260–780°C with an estimated mass losses of 61.76 % (theoretical 61.58 %) and 56.0 % (theoretical 55.59 %) for the Fe(III) and Co(II) complexes, respectively, leaving behind the metal chloride (in case of Fe(III)) or metal carbonate (in case of Co(II)) as the residue.

The Ni(II) complex of the general formula $[Ni(HL)_2]H_2O$ gives a four-stage decomposition process. The first stage (from 28–200°C) may represent the loss of water molecule of hydration (estimated mass loss 3.38 %, theoretical 3.29 %). The activation energy for this dehydration step is equal to 50.93 kJ mol^{-1}. The second (from 200–310°C), the third (from 310–390°C) and the fourth (from 390–585°C) stages may be due to the decomposition of the two ligand molecules leaving nickel oxide as the residue. The mass losses for these temperature ranges are 9.54 % (theoretical 9.47 %), 14.29 % (theoretical 14.39 %) and 52.18 % (theoretical 52.10 %), respectively.

The TG and DTG plots of the Cu(II) complex are represented in Fig. 1. The thermolysis curves of $[M(HL)(H_2O)](OAc)$ (where M = Cu(II) and Zn(II) ions) complexes show mass loss in the temperature range of 150–845 and 130–730°C for Cu(II) and Zn(II) complexes, respectively. The decomposition processes occur in three steps and the overall mass losses amount to 79.49 % (theoretical 78.89 %) and 75.24 % (theoretical 75.40 %) for Cu(II) and Zn(II) complexes, respectively, which may be attributed to the loss of the acetate group (CH_4 and CO_2), coordinated water and ligand molecules leaving metal oxide as a residue.

The curves of $[Cd(HL)(H_2O)]Cl$ complex shows that at a temperature of 25–140°C, the estimated mass loss of 8.46 % (theoretical 8.84 %) may be due to the escape of Cl atom [22]. The ligand moiety and coordinated water molecules start dissociation at 140–310 and 310–630°C leaving behind the metal oxide as residue of decomposition. The mass losses corresponding to these temperature ranges are 17.50% (theoretical 17.43 %) and 47.65% (theoretical 47.82%), respectively.

Table 2 Thermoanalytical results (TG, DTG) of salicylidene-2-aminobenzimidazole complexes

Complex	TG range/ °C	DTG_{max}/ °C	Mass loss/%	Total mass loss/%	Assignment
			Estimated (Calcd.)		
$[Fe(HL)(H_2O)_3](Cl)_2\cdot3H_2O$	25–170	102	14.45 (14.23)		Loss of $3H_2O$
	175–545	335	28.71 (28.21)		Loss $3H_2O$ (coord.), $2HCl$ and $1/2O_2$
	545–970	825	43.35 (43.42)	86.51 (85.86)	Loss of $C_{14}H_{10}N_3$ leaving metal oxide residue
$[Co(H_2L)(H_2O)_3](Cl)_2\cdot3H_2O$	25–260	119	17.73 (17.65)		Loss of $3H_2O$
	260–550	368	10.53 (10.59)		Loss of $3H_2O$ (coord.)
	550–780	683	46.68 (46.27)	74.94 (74.51)	Loss of $C_{14}H_{11}N_3O$ leaving metal chloride residue
$[Ni(HL)_2]\cdot H_2O$	28–200	160	3.35 (3.29)		Loss of H_2O
	200–310	276	9.54 (9.47)		Loss of C_2H_2
	310–390	343	26.29 (26.14)		Loss of $C_8H_5N_3$
	390–585	431	52.18 (52.10)	91.39 (91.0)	Loss of $C_{18}H_{11}N_3O$ leaving metal oxide residue

Table 2 Continued

Complex	TG range/ °C	DTG$_{max}$/ °C	Mass loss/%	Total mass loss/%	Assignment
			Estimated (Calcd.)		
[Cu(HL)(H_2O)](OAc)	150–300	260	11.38 (11.69)		Loss of CO_2
	300–425	355	9.36 (9.03)		Loss of H_2O (coord) and CH_4
	425–845	590	58.31 (58.17)	79.05 (78.89)	Loss of $C_{14}H_9N_3$ leaving metal oxide residue
[Zn(HL)(H_2O)](OAc)	130–280	245	20.57 (20.37)		Loss of H_2O (coord.), CO_2 and CH_4
	280–480	396	27.38 (27.78)		Loss of $C_6H_5N_2$
	480–730	620	27.29 (27.25)	75.24 (75.40)	Loss of C_8H_4N leaving metal oxide residue
[Cd(HL)(H_2O)]Cl	25–140	85	8.46 (8.84)		Loss of 1/2Cl_2
	140–310	243	17.50 (17.43)		Loss of H_2O (coord.) and C_2H_4
	310–630	520	47.65 (47.82)	73.61 (74.09)	Loss of $C_{12}H_5N_3$ leaving metal oxide residue

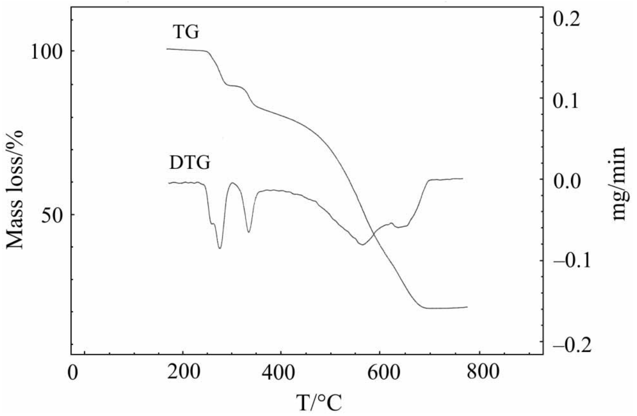

Fig. 1 TG and DTG curves of Cu–SABI complex

In general, the stages of thermal decomposition of the complexes can be written as shown:

$$[M(HL)_z(H_2O)_x](A)_n\ .yH_2O \xrightarrow[\text{Dehydration}]{50\text{–}205\ ^\circ C} [M(HL)_z(H_2O)_x](A)_n + yH_2O$$

where M= Fe(III) and Co(II)[z=1, x=3, A=Cl, n=2, y=3]=Ni(II)[z=2, x=0, A=0, n=0, y=1]

For the anhydrous complexes:

$$[M(HL)_z(H_2O)_x](A)_n \xrightarrow{25\text{–}550\ ^\circ C} \text{Intermediate (unstable)}$$

$$\text{Intermediate} \xrightarrow[\text{final decomposition}]{550\text{–}970\ ^\circ C}$$

Metal chloride ; in case of Fe(III) complex
or Metal carbonate ; in case of Co(II) complex
or Metal oxide; in case of Cu(II), Ni(II), Zn(II) and Cd(II) complexes.

The natures of the intermediates formed in the other subsequent steps are proposed and they give violent decomposition to give the respective metal oxides or chloride or carbonate as the final products.

Calculation of activation thermodynamic parameters of the decomposed complexes

The thermodynamic activation parameters of decomposition processes of dehydrated complexes namely activation energy (E*), enthalpy (ΔH*), entropy (ΔS*) and free energy of decomposition (ΔG*), were evaluated graphically by employing the Coats-Redfern method [23]. Figure 2 represents the Coats–Redfern plots of the decomposition steps of Cu-SABI complex. The data are summarized in Table 3. According to the kinetic data obtained from DTG curves, all the complexes have entropy which indicates that activated complexes have more ordered systems than reactants.

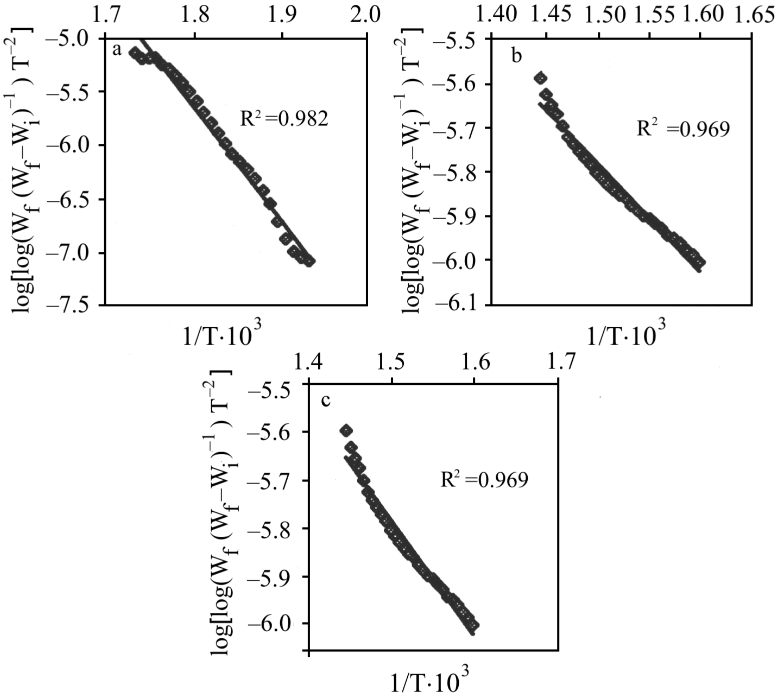

Fig. 2 Coats–Redfern plots of a, b and c decomposition steps of Cu(II)–SABI complex

From Table 3, it is obvious that, the nickel complex shows a higher thermal stability than those of copper. This can be discussed in terms of repulsions among electron pairs in the valence shell of the central ion. The higher electronegativity of copper compared to that of nickel leads to a higher repulsion between bonding pairs in the valence shell of copper ion giving lower stability [6, 24]. Based on the activation energy values, Zn(II) complex shows a lower thermal stability than Cd(II) complex. This can be discussed in terms of repulsion among electron pairs in the valence shell of the central ion. Both zinc and cadmium ions in the investigated complexes have multiple bonding (four bonds) in their valence shells. But due to the small ionic size of zinc than that of cadmium leads to a higher repulsion between the bonding pairs in the valence shell of zinc which in turn alters the bond angles from those of ideal tetrahedral, giving a lower stability [19, 24]. The lower thermal stability of the cobalt complex may be attributed to the higher repulsion between the multiple-bonding electron pairs (six bonds) in the valence shell of cobalt, as well as to the higher repulsion obtained by the non-bonded pairs of electrons on the axial donating oxygen of the water molecule and the bonded electrons [19].

Table 3 Thermodynamic data of the thermal decomposition of salicylidene 2-aminobenzimidazole complexes

Complexes	Decomposition range/°C	E^*/ kJ mol^{-1}	A, Arrhenius factor/s^{-1}	ΔS^*/ kJ mol^{-1} K^{-1}·10^{-3}	ΔH^*/ kJ mol^{-1}	ΔG^*/ kJ mol^{-1}
$[Fe(HL)(H_2O)_3](Cl)_2\cdot 3H_2O$	50–170	45.76	$1.11\cdot 10^{5}$	–6.55	70.72	80.30
	175–545	107.2	$1.85\cdot 10^{9}$	–7.95	105.6	107.6
	545–970	90.44	$1.37\cdot 10^{7}$	–14.05	83.58	95.16
$[Co(H_2L)(H_2O)_3]Cl_2\cdot 3H_2O$	25–260	40.24	$3.12\cdot 10^{5}$	–15.89	39.26	41.13
	260–550	53.66	$6.45\cdot 10^{6}$	–14.04	50.44	55.86
	550–780	167.7	$9.21\cdot 10^{7}$	–11.92	162.2	170.0
$[Ni(HL)_2]\cdot H_2O$	28–200	50.93	$1.18\cdot 10^{5}$	–17.22	49.0	51.90
	200–310	138.0	$3.99\cdot 10^{12}$	–10.34	136.3	136.4
	310–390	270.2	$1.39\cdot 10^{22}$	–21.38	267.3	260.0
	390–585	413.0	$7.86\cdot 10^{29}$	–39.0	409.0	392.0
$[Cu(HL)(H_2O)](OAc)$	150–300	59.40	$1.56\cdot 10^{5}$	–17.40	57.16	61.84
	305–425	201.4	$1.75\cdot 10^{6}$	–15.23	198.5	203.7
	425–845	112.1	$4.36\cdot 10^{5}$	–17.16	107.2	117.3
$[Zn(HL)(H_2O)]OAc$	130–280	39.85	$3.02\cdot 10^{5}$	–15.58	39.15	40.47
	280–480	45.80	$1.02\cdot 10^{6}$	–15.42	43.78	47.52
	480–730	125.5	1.47·107	–13.53	121.1	128.25
$[Cd(HL)(H_2O)]Cl$	25–140	124.2	$3.67\cdot 10^{10}$	–8.87	121.8	123.3
	140–310	165.5	$1.03\cdot 10^{10}$	–6.83	152.8	155.9
	310–630	152.1	$3.77\cdot 10^{7}$	–12.75	147.0	155.0

Structural interpretation

From all of the above observations, the structure of these complexes may be given in accordance with those previously reported [1, 2, 6, 8–11], which indicate that the Schiff base ligands coordinated to metal ions through the N, O, N or N, O, S system according to the structure of the Schiff base used. According to the above explanation, the structure of SABI-di- and tri-valent metal ions is given in Fig. 3.

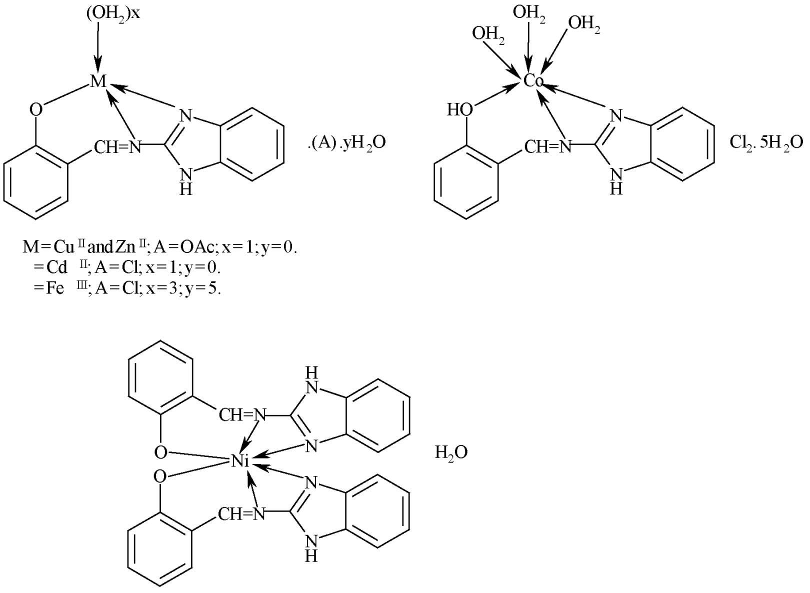

M=Cu^{II} and Zn^{II}; A=OAc; x=1; y=0.
=Cd^{II}; A=Cl; x=1; y=0.
=Fe^{III}; A=Cl; x=3; y=5.

Fig. 3 Structural formula of SABI–metal complexes

Conclusion

The design and synthesis of a new tridentate Schiff base ligand derived from 2-amino-benzimidazole and salicylaldehyde for use in tetrahedral or octahedral molecular templates have been successfully demonstrated. The synthesis of the ligand and its complexes proved to be as straightforward as expected, giving high yields of either the free ligand or its complexes in simple, one-pot reactions. As anticipated, the ligand coordinates equatrially to four- or six- coordinate transition metal ions to give square planar (Cu(II)), tetrahedral (Zn(II) and Cd(II)) and octahedral (Co(II), Ni(II) and Fe(III)) environment, around the metal ion anchor. In a similar mannar to those previously reported for the Schiff base complexes of O, N, N or O, N, S tridentate ligands [5, 6, 25], it may be possible to try to test these Schiff base complexes as antibacterial, antitubercular, antifungal and anticoagulant activity.

References

1 A. Z. El-Sonbati, Trans. Met. Chem., 16 (1991) 45.

2 A. A. Soliman, J. Therm. Anal., 63 (2001) 221.

3 A. F. Petrovic, D. M. Petrovic, V. M. Leovac and M. Budimir, J. Therm. Anal. Cal., 58 (1999) 589.

4 I. Ivanovic, K. Andjelkovic, V. M. Leovac, Lj. Klisarov, M. Lazarevic and D. Minic, J. Thermal Anal., 46 (1996) 1741.

5 Z. M. Zaki, S. S. Haggag and A. A. Soayed, Spectroscopy Letters, 31 (1998) 757.

6 C. K. Bhaskare and P. P. Hankare, J. Ind. Chem. Soc., 72 (1995) 585.

7 W. S. Sawodny and M. Riederer, Angew. Chem., Int. Edn. Engl., 16 (1977) 859.

8 T. L. Samuel and M. K. Stanley, Trans. Met. Chem., 25 (2000) 415.

9 A. Harry, B. Rufina, E. F. David, M. Alejandro, E. S. Sharon and V. Laura, J. Chem. Soc., Dalton Trans., 23 (1999) 4131.

10 I. C. Santos, M. Vilas-Boas, M. F. M. Piedade, C. Freire, M. T. Duarte and B. De Castro, Polyhedron, 19 (2000) 655.

11 (a) H. M. J. Hendriks, P. J. M. W. L. Birker, G. C. Verschoor and J. Reedijk, J. Chem. Soc., Dalton Trans., 623 (1982). (b) J. van Rijn, W. L. Driessen, J. Reedijk and J. M. Lehn, Inorg. Chem., 23 (1984), 3584. (c) A. W. Addison, T. N. Rao, J. Reedijk, J. van Rijn and G. C. Verschoor, J. Chem. Soc., Dalton Trans., 1349 (1984). (d) M. F. Summers, J. van Rijn, J. Reedijk and L. G. Marzilli, J. Am. Chem. Soc., 108 (1986), 4254. (e) J. M. Mdoney, M. Glogowski, D. F. Rohrbach and F. L. Urbach, Inorg. Chim. Acta, 127 (1987), L33, (f) Y. Nishidi, H. Shimo, H. Maehara and S. Kida, J. Chem. Soc., Dalton Trans., 1954 (1985). (j) J. van Rijn, 'Copper Chelates with Imidazole-Containing Ligands' , Ph.D. Thesis, Leiden University, The Netherlands, (1985). (h) K. Takahashi, E. Ogawa, N. Oishi, Y. Nishida and S. Kida, Inorg. Chim. Acta, 66 (1982) 97.

12 S. K. Sahni, W. L. Driessen and J. Reedijk, Inorg. Chim. Acta, 154 (1988) 141.

13 P. Hodge, in P. Hodge and D. C. Sherrington (eds.), 'Polymer-Supported Reactions in Organic Synthesis', Wiley, New York p. 457 (1980).

14 G. G. Mohamed, N. E. A. El-Gamel and F. A. Nour El-Dien, Synth. React. Inorg. Met.-Org. Chem., 31 (2001) 347.

15 S. R. R. Thomas and G. Parameshwaran, J. Ind. Chem. Soc., 69 (1992) 117.

16 J. R. Dyer, Applications of Absorptions Spectroscopy of Organic Compounds; Prentice-Hall of India, New Delhi (1984); A. C. Hiremath, Z. S. Qureshi, K. M. Reddy and M. B. Halli, Indian J. Chem. Soc., Sec. A, 30 (1991) 293.

17 J. A. Dean, Lange`s Handbook of Chemistry: 14th Edition, McGraw-Hill, New York 1992.

18 M. S. Masoud, A. M. Hindawy and A. A. Soayed, Trans. Met. Chem., 16 (1991) 372.

19 Z. M. Zaki and G. G. Mohamed, Spectrochim. Acta (Part A), 56 (2000) 1245.

20 M. M. Khalil, A. H. H. El-Ghandour, M. Mostafa and M. M. Shoukry, Polyhedron, 13 (1994) 3295.

21 Y. M. Essa, H. M. Abdel-Fattah and A. A. Soliman, J. Therm. Anal., 42 (1994) 1175.

22 S. L. Stefan, J. Therm. Anal., 42 (1994) 1299.

23 A. W. Coats and J. P. Redfern, Nature, 20 (1964) 68.

24 A. M. Donia, M. M. Gouda, M. I. Ayad and H. A. El-Boraey, Thermochim. Acta, 194 (1992) 155.

25 V. D. Athawale and S. S. Nerkar, Monatsh. Chem., 131 (2000) 267.